Aqueous TiO_2 Nanoparticles React by Proton-Coupled Electron Transfer

Jennifer L. Peper, Noreen E. Gentry, Benjamin Boudy, and James M. Mayer*

Department of Chemistry, Yale University, New Haven, Connecticut 06520-8107, United States

james.mayer@yale.edu

ABSTRACT:

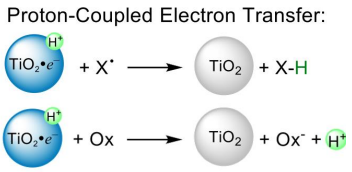

Redox reactions of aqueous colloidal TiO_2 4 nm nanoparticles (NPs) have been examined, including both citrate-capped and uncapped NPs (*c*-TiO_2 and *uc*-TiO_2). Photoreduction gave stable blue colloidal *c*-TiO_2^R NPs with 10-60 electrons per particle. Equilibration of these reduced NPs with soluble redox reagents such as methylviologen (MV^{2+}) provided measurements of the colloid reduction potential as a function of pH. The potentials of *c*-TiO_2 from pH 2-9 varied linearly with pH, with a slope of –60 ± 5 mV/pH. Estimates of the potential at pH 12 were consistent with extrapolating that line to high pH. The reduction potentials did not correlate with the zeta potentials (ζ) or the surface charge of the NPs across this pH range. Similar reduction potentials were observed for *c*- and *uc*-TiO_2 at low pH even though they have quite different ζ potentials. These results show that the common surface-charging explanation of the pH dependence is not tenable in these systems. Oxidation of reduced *c*-TiO_2^R with the electron-transfer oxidant potassium triiodide (KI_3) occurred with a significant drop in pH, showing that protons were released when the electrons were removed from the NPs. Smaller pH drops were observed for the proton-coupled electron transfer (PCET) reagents O_2 (air) and 4-MeO-TEMPO (4-methoxy-2,2,6,6-tetramethyl-piperine-1-oxy radical). The difference in the number of protons released with KI_3 vs. O_2 and 4-MeO-TEMPO was roughly one proton per electron removed. Thus, the thermodynamically preferred reactivity of these colloidal TiO_2 NPs is PCET over the pH 2-13 range studied. The measured redox potentials refer to the chemical process $TiO_2 + H^+ + e^- \rightarrow TiO_2{\bullet}e^-,H^+$, and therefore they do not correspond with an electronic energy such as a conduction band edge or flat band potential. The $1e^-/1H^+$ stoichiometry means that the reduction TiO_2 reduction potentials correspond to a TiO_2–H bond dissociation free energy (BDFE), determined to be 49 ± 2 kcal mol^{-1}. The PCET description is consistent with the pH dependence of $E(TiO_2/TiO_2{\bullet}e^-,H^+)$, the release of protons upon oxidation, the lack of correlation with ζ potentials, the similarity of capped and uncapped NPs, and the small change in the potential and BDFE from the first to the last electron/proton pair (H-atom) removed. This behavior is suggested to be the norm for redox-active oxide/water interfaces.

Introduction

The ability of titanium dioxide (TiO_2) and other metal oxides to undergo and perform redox chemical reactions is central to their applications in energy conversion, pollution remediation, and many other technologies.[1-9] Such redox reactivity has been studied with bulk solids, with thin films, and with nanoscale materials of various dimensions. Redox processes at solid/solution interfaces, typically referred to as interfacial electron transfers (ETs), have resulted in a deep understanding of charge carriers, charge injection, and charge transport in these complex materials. However, there are many aspects of metal oxide reactivity that are difficult to explain within a pure-ET paradigm of reactivity. For instance, the band edge energies of many semiconducting metal oxide electrodes at aqueous interfaces shift by roughly –60 mV per pH unit.[2,10,11] Perhaps also surprising is the ability of many of these material to reach very high levels of charge storage.[4] The colloidal TiO_2 nanoparticles (NPs) that are the focus of this study can be photochemically reduced to the level of several hundred electrons in a single ~4 nm diameter NP, to $>10^{21}$ e^- cm^{-3} (>3% of the Ti^{4+} reduced).[4,7,12-14] These reduced colloids, TiO_2^R, have long-term chemical and colloid stability.

Traditional explanations of these common features of metal oxide reactivity are centered around the buildup of charge at or near the materials surface. The stability of highly reduced particles has been justified by the large capacitance of the double layer surrounding each particle.[4] The pH dependence of metal oxide thermochemistry is traditionally ascribed to changes in surface charge via acid-base chemistry of surface oxide groups.[10,15] However, the relatively narrow range of surface oxide pK_a's and the limited number of surface sites cannot explain the 64 mV/pH dependence of TiO_2 electrodes over 10^{25} in proton activity, as Hupp *et al.* concluded more than twenty years ago.[16-19]

Thus, the reactivity of oxide/aqueous interfaces are increasingly understood to involve the stoichiometric coupling of ET with proton transfer to the surface or proton intercalation into surface layers.[16-28] This is the dominant model, for instance, for metal oxide 'pseudocapacitors'.[29] In this model, the near -60 mV per pH shift of band edge energies is analogous to the -60 mV/pH Nernstian dependence of $1e^-/1H^+$ proton-coupled electron transfer (PCET) reactions of well-defined molecules in solution.[30-32] In fact, Pourbaix's famous Atlas from 1963 indicates -60 mV/pH behavior for many oxide/water interfaces.[33,34] While there is good precedent for this PCET paradigm, it is still the minority view to an ET-centric perspective.

The studies presented here show that the redox chemistry of colloidal aqueous TiO_2 NPs not only can follow this PCET paradigm, but *it is their thermochemically preferred mode of reaction*. This work examines the stoichiometry and equilibrium positions of the reactions of TiO_2^R with well-defined oxidants; future studies will probe the kinetics and mechanism(s) of the PCET reac-

tions. We report that TiO_2^R colloids oxidized with *electron-only* oxidants become more acidic than those oxidized with *proton-coupled oxidants*. Evaluation of the pH difference between the oxidized colloids demonstrates that removal of each additional electron from the NPs releases roughly one proton to the colloid solution.

A near -60 mV per pH dependence of the reduction potential of the colloidal TiO_2^R NPs ($E(TiO_2^{Ox/R})$) over a wide pH range is shown by equilibration with soluble reagents. This has previously been demonstrated in TiO_2 thin film electrodes[2,16] and for colloidal TiO_2 nanoparticles both in a study by Grätzel *et al.*, between pH 2 and 3[35] and in a pulse-radiolysis study by Mićić, Nozik *et al.*[15] We examine the traditional interpretation of the pH-dependence of semiconductor reactivity—as a surface protonation (acid-base) effect—using ζ-potential measurements as a proxy for the TiO_2 NP surface charge.[2,36,37] Together, these results show that the redox chemistry of colloidal TiO_2 NPs is an obligatory PCET process under these conditions. The data indicate a roughly 1:1 stoichiometry of protons to electrons, so TiO_2^R can be defined more specifically as $TiO_2{\bullet}e^-,H^+$ or TiO_2H_x.

Results

I. Synthesis, characterization, and photochemical reduction of TiO_2 nanoparticles

Anatase titanium dioxide NPs (diameter = 4 ± 1 nm by TEM) were synthesized via hydrolysis of titanium(IV) tetrachloride as previously described.[12-14] The resulting white solid was re-suspended in neutral 18 MΩ cm water (3g solid L^{-1}) to give a transparent colloid at pH 2.0-2.3. This clear suspension of *uncapped* NPs (*uc*-TiO_2) was electrostatically stabilized at low pH 2.0–2.8 and high pH > 9.5; NP agglomeration was observed from ~pH 3 – 9.5. By TEM and ICP-MS, the colloids were determined to be ~30 μM in NPs, ~30 mM in Ti (~1,000 Ti/NP). The NPs were further characterized by p-XRD, DLS, and UV-visible spectroscopy. See SI-Section 1 for details.

To extend the range of stable pH values beyond that of *uc*-TiO_2, a few carboxylate capping ligands were explored to stabilize the NPs from agglomeration. The addition of citric acid monohydrate (4-20 mM) to *uc*-TiO_2 resulted in a slight decrease in the colloid pH and visible aggregation of the nanoparticles, resulting in a cloudy white solution. Subsequent addition of base, aqueous tetramethylammonium hydroxide (NMe_4OH) solution, gave way to transparent citric acid capped TiO_2 colloids (*c*-TiO_2) that were stable from pH 3 – 13.5. Proline and arginine were also assessed as potential stabilizing ligands, but neither extended the pH range for stable colloids. Most of the studies in this paper used these *c*-TiO_2 colloids. Some experiments were performed in D_2O and in these instances pD is reported instead of pH, using standard literature corrections (see SI-Section 1.7).[38-41]

Phase analysis light scattering (PALS) was used to evaluate the zeta potentials (ζ potentials) of fully oxidized *uc*- and *c*-TiO_2 across a wide pH range (SI-Section 1.6). The ζ potential is the electrical potential at the hydrodynamic slipping plane of a colloidal NP. While the ζ potential is not the same as the charge at the surface of the NP, the two parameters parallel each other.[2,36,37] Large positive or negative ζ potentials are indicative of stable colloids, while a ζ potential of 0 reflects the point of zero charge.

uc-TiO_2 exhibit ζ potentials of +40 mV and –50 mV at low and high pH, ~2.2 and ~12 respectively. These values and the inversion of the sign of the charge were reversible over multiple cycles (Figure S5). This indicates that the *uc*-TiO_2 surface at low pH was large and positive, due to surface protonation, while they are large but of opposite sign at high pH. The large surface charges are responsible for the stability of the colloids. *uc*-TiO_2 agglomeration was observed closer to neutral pH, because TiO_2 surfaces have their point of zero charge between pH 3.5-7.5.[3,6,42,43]

The *c*-TiO_2 colloids, in contrast, had negative ζ potentials throughout the pH range 3-13.5, with ζ values between –30 and –50 mV (Figure 1; SI-Section 1.6). This is consistent with prior studies of such colloids.[44] The negative ζ potential for the *c*-TiO_2 indicates that citrate anions are closely associated with the nanoparticle surface. Thus, the stability of the *c*-TiO_2 results over a wide pH range results from the electrostatic net negative charge of the nanoparticle surface with its citrate ligands.

Most of the experiments reported in this study used photochemically reduced, thermally equilibrated NPs (TiO_2^R). NP reduction was achieved via anaerobic UV-photolysis, similar to many previous reports (SI-Section 2).[12-14,42,45-48] The added electrons in the TiO_2^R turned the colloids blue in color, an optical contrast to the colorless oxidized form. The number of electrons in each colloid suspension were quantified via optical titrations with various oxidants (SI-Section 2.1).[13] Methanol (0.1 M) was the sacrificial reductant for *uc*-TiO_2 while citric acid (4-20 mM) served that function for the *c*-TiO_2 (pre-photolysis pH ~4-5.5). Citrate photolysis was ~100 times faster than that with methanol (minutes vs. hours), consistent with the higher surface binding affinity of citrate relative to methanol.[43] The reduced NP colloids were stable for many hours under inert atmosphere but reacted quickly with O_2, resulting in the disappearance of the blue coloration. Thus, all experiments with TiO_2^R were conducted under a nitrogen atmosphere inside a glovebox, with the exception of the O_2 reactions which were conducted on the benchtop.

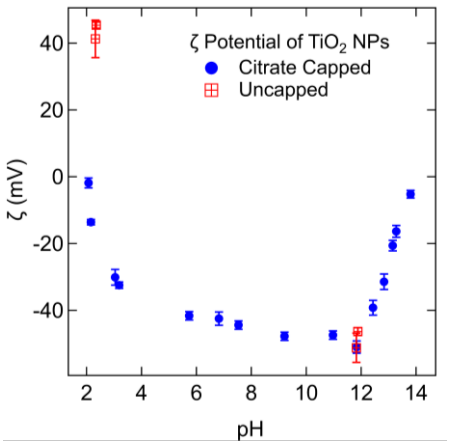

Figure 1. ζ potential measurements using phase analysis light scattering (PALS) are shown of citrate-capped *c*-TiO_2 colloids (blue circles) and uncapped *uc*-TiO_2 (red squares) as a function of pH.

II. ET versus PCET Oxidation of Reduced Colloids TiO_2^R

Various oxidants stoichiometrically remove all of the added electrons in TiO_2^R, including potassium triiodide (KI_3), 4-MeO-TEMPO (4-methoxy-2,2,6,6-tetramethyl-piperine-1-oxy radical) and O_2 (air), as indicated by optical spectroscopy (SI-Section 2.2).[14] While KI_3 is an outer sphere electron-only oxidant, 4-MeO-TEMPO is a well-established hydrogen atom or PCET ($1e^-/1H^+$) acceptor. 4-MeO-TEMPO reacts with TiO_2^R to give 4-MeO-TEMPO-H (or its protonated form at low pH) (Figure S7B).[13,14,31,49] Similarly, the proton-coupled reduction of O_2 by TiO_2^R is established in the literature.[12,50] Optical spectroscopy was used to account for TiO_2^R based electrons, while pH was used to assess the approximate proton concentration of the solution ($pH = -\log_{10}[\alpha_{H^+}] \approx -\log_{10}[H^+]$). The approach and limitations of

using the direct change in pH (ΔpH) to determine solution proton concentration (Δ[H^+]) are discussed further below.

A batch of *c*-TiO_2 was photochemically reduced, equilibrated, and separated into aliquots (0.82 mM e^-, pH 8.5). To probe whether these ET reactions are coupled to proton transfer (PT), the colloid pH was examined before and after oxidations with KI_3, 4-MeO-TEMPO, and O_2 (air). The final pH of the aliquot oxidized with KI_3 was 7.5, while the aliquots oxidized by 4-MeO-TEMPO and O_2 were 8.2 and 8.1, respectively (Scheme 1). The change in pH with these oxidants was assessed for *c*-TiO_2^R at other pHs (5.55 – 10) and KI_3 treated samples were always 0.5–1.0 pH units more acidic than 4-MeO-TEMPO or O_2 oxidized samples (SI-Section 3.2, Table S2). The interpretation of this pH drop is given in the following paragraphs.

Scheme 1. Oxidations of photochemically reduced, citrate-capped TiO_2 NPs (TiO_2^R) by KI_3, 4-MeO-TEMPO, and O_2 (air).[a]

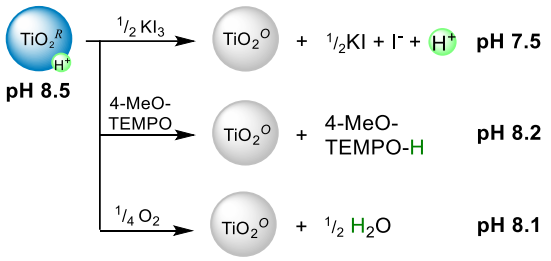

[a] TiO_2^R initially pH 8.5, 0.82 mM e^-, ~30 μM NPs, 5.6 mM citric acid, prepared by addition of aqueous NMe_4OH to *c*-TiO_2^R at pH 6.1. KI_3: 29 mM KI, 7.8 mM ½I_2; 4-MeO-TEMPO: 15 mM, O_2: air, excess. [e^-] in reduced TiO_2 were quantified via optical titrations with KI_3 (SI-Section 2.2).

The number of protons per electron released from the NPs upon oxidation is challenging to determine from the ΔpH in Scheme 1 because the buffering capacity of the TiO_2 plus citrate solution is not well defined (SI-Figure 3.3). The complications include the amphoteric nature of the TiO_2 surface, the shifts in citric acid pK_as upon binding to TiO_2, the possible shifts in the number and ligation mode of citrate with pH, and the photooxidation products of citric acid that also buffer the solution (SI – Figure 3.3, SI-Section 3.4).[6,10,43,44]

Therefore, the Δ[H^+] was quantified empirically: A photochemically reduced colloid *c*-TiO_2^R (pH 8.55, 0.8 mM e^-), was split into two aliquots and oxidized with KI_3 or O_2 (Figure 2A). Then 2 mL of the O_2-oxidized colloid were titrated with aqueous HCl (49 mM), to measure the concentration of protons required to reach the lower pH of the KI_3-oxidized colloid. The titration curve (Figure 2B, red line) showed that 1.85 μmol H^+ (0.9 mM) were required to reach the pH of the KI_3-oxidized colloid (pH 7.53) (black dashed lines). This 1.85 μmol H^+ is close to the 1.6 μmol of e^- in the starting aliquots: the ratio of protons released to electrons removed was 1.15:1. A similar experiment (SI-Section 3.5) gave a ratio of 0.89:1. Thus, TiO_2^R can be identified as having a stoichiometry close to TiO_2•e^-,H^+ (1.02 ± 0.13 H: e^-).

Other, smaller pH changes were observed in a number of experiments with *c*-TiO_2. The initial photolysis of *c*-TiO_2, for instance, always gave a rise in pH. This is likely due in part to the uptake of protons by *c*-TiO_2 upon reduction, but quantitative analysis is complicated by the photo-oxidation of citrate ions (the sacrificial reductant). Oxidation of citrate^{3-} reduces its concentration and forms 3-oxoglutarate, carbonic acid (H_2CO_3), CO_2, and further products such as acetone (SI-Section 2.1, SI Section 3.4).[47,51] All of these changes in solution composition as well as changes in surface ligation can affect the pH. Changes in surface ligation may also contribute to the small drop in pH upon oxidation of *c*-TiO_2^R with PCET reagents. This would seem to indicate that each electron is transferred with roughly one proton, as has been observed in some other oxide systems (cf., [52-54]).

Overall, the larger pH trends of these three reactions indicate that TiO_2^R is a proton-coupled reductant rather than a simple electron transfer agent. The treatment of TiO_2^R with the ET-only oxidant I_3^- results in the release of protons to the aqueous solution and a decrease in colloid pH. In contrast, PCET oxidants accept electrons *and protons*, mitigating the acidification of the solution upon oxidation (Scheme 1 and Figure 2A). Photocharging is roughly the reverse, with the NPs taking up protons upon reduction (protons are released by the photo-reductant, citrate or MeOH).

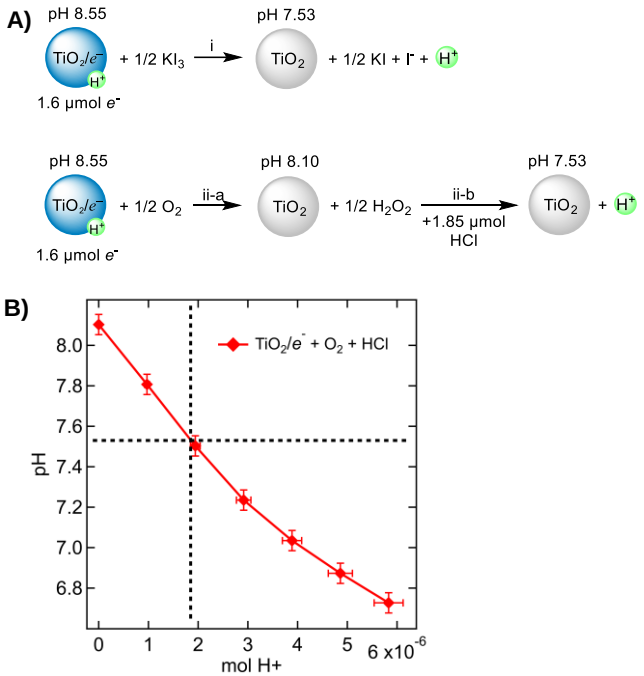

Figure 2. A) Schematic of KI_3 (i) and O_2 (ii-a) oxidations of *c*-TiO_2^R NPs (2 mL, 1.6 μmol [0.8 mM] e^-, ~30 μM NPs, 5.2 mM citric acid.). **B)** Acid titration (aqueous HCl, 49 mM) of the O_2-oxidized *c*-TiO_2. Black dashed lines mark the final pH of the KI_3 oxidized colloid and its intersection with the titration curve. The pH of the O_2-oxidized colloid was equal to that of the KI_3-oxidized colloid upon addition of 1.85 μmol of HCl (**A**, ii-b).

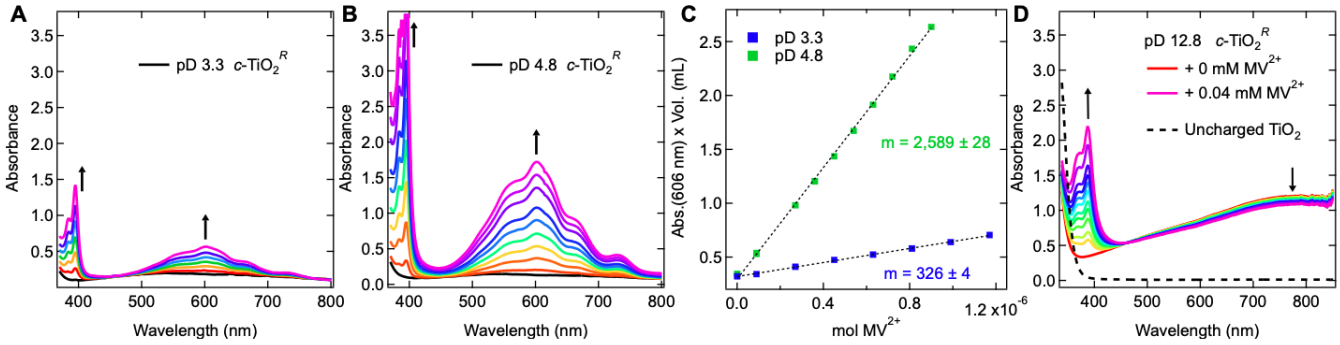

Figure 3. Optical spectra for titration of *c*-TiO_2^R with MV^{2+} at pD 3.3 (**A**) and pD 4.8 (**B**) (in D_2O, 1.0 mM e^-, ~30 µM NPs, 17 mM citric acid), showing the growth of the $MV^{\bullet+}$ spectrum. (**C**) A plot of Absorbance 606 nm × Volume as a function of mol MV^{2+} for the **A** and **B** titrations. The slopes of these lines, used in eq 3 to determine the fraction of MV^+ (δ), have been included. The absorbances at mol MV^{2+} = 0 are due to the *c*-TiO_2^R. (**D**) Optical spectra following the initial (ca. 10%) titration of *c*-TiO_2^R with MV^{2+} at pD 12.8 (in D_2O, 1.0 mM e^-, ~30 µM NPs, 17 mM citric acid). The growth of the peak at 385nm and the lack of the MV^+ peak at 606 nm indicate quantitative reduction of MV^{2+} to MV^0.

III. E($TiO_2^{Ox/R}$) as a function of pH

To further probe the involvement of protons in redox reactions of the TiO_2 colloids, we determined their reduction potentials $E(TiO_2^{Ox/R})$ as a function of pH. Thermally equilibrated, photochemically reduced TiO_2^R was titrated with various soluble oxidants (Ox/Red). At equilibrium, the non-standard reduction potentials (*E*) of the two couples in solution are equal (eq 1), similar to previous equilibration studies.[15,35] Thus, in each titration experiment, the reduction potential of TiO_2 was determined from the equilibrated potential of the Ox/Red couple, *E*(Ox/Red), via the Nernst equation (eq 2).

$$E(TiO_2^{Ox/R}) = E(\text{Ox/Red}) \quad (1)$$

$$E(\text{Ox/Red}) = E°(\text{Ox/Red}) - 59\text{ mV}\log\frac{[\text{Red}]}{[\text{Ox}]} \quad (2)$$

$$\text{A} \times \text{Vol} = (\text{Ox mol}) \times \delta(\varepsilon_{\text{Red}} - \varepsilon_{TiO_2^R}) \times l \quad (3)$$

The equilibration experiments were done by photochemically reducing the colloid and then adjusting the pH of thermally equilibrated TiO_2^R via the addition of NMe_4OH. The spectral changes upon pH change were rapid for *uc*-TiO_2^R but occurred over ~5 hours for *c*-TiO_2^R (SI-Section 3.1). Raising the pH resulted in a reversible increase and a redshift in the optical density, with a peak at 780 nm evident at high pH (Figure S8A, Figure S9A). Following the pH adjustments and full equilibration of the solutions, the TiO_2^R was titrated with various oxidants and monitored by optical spectroscopy. The fraction of reduced oxidant (δ) was determined from the measured change in absorbance as a function of moles oxidant (Ox mol) titrated and the known molar extinction coefficients of Red (ε_{Red}) and TiO_2^R ($\varepsilon_{TiO_2^R}$) (eq 3, where *l* is path length).

An example of this analysis is present in **Figure 3**A-C. The addition of *sub*-stoichiometric methyl viologen (MV^{2+}) to *c*-TiO_2^R (pD 3.3 and pD 4.8) resulted in the appearance of signature MV^+ optical peaks at 395 and 606 nm (**Figure 3**A-B). The change in {Absorbance(606nm)×volume} as a function of titrated MV^{2+} (plotted in **Figure 3**C) gives the fraction (δ) of MV^{2+} reduced to MV^+. For the pD 3.3 experiment, the slope—the absorbance growth of Red (MV^+ at 606 nm) as a function of titrated MV^{2+}—is only 2.5% of $\varepsilon_{MV+} - \varepsilon_{TiO2R}$ (≈ 13,500 M^{-1} cm^{-1}) indicating that only 2.5% of the added MV^{2+} is reduced to MV^+ by TiO_2^R. This result implies, from eqs 1 and 2, that $E(TiO_2^{Ox/R})$ is 94 mV more positive than the standard potential of $MV^{2+/+}$, -0.446 V. In contrast, the steeper slope of the pD 4.8 titrations in **Figure 3**C indicates that 20% of the added MV^{2+} is reduced to MV^+ under these conditions. Thus pD 4.8 *c*-TiO_2^R is 60 mV more reducing than the same colloid at pD 3.3 (-0.408 vs. -0.348 V) and only 38 mV less reducing than $E(MV^{2+/+})$ (Table 1).

Titrations of *c*-TiO_2^R with MV^{2+} under highly basic conditions gave very different results. The reaction of *sub*-stoichiometric MV^{2+} and pD 12.8 *c*-TiO_2^R gave a singular absorbance peak below 400 nm. These results imply the complete two-electron reduction of MV^{2+} to form MV^0 (**Figure 3**D). The full conversion of this reaction indicated that $E_{pD12.8}(TiO_2^{Ox/R})$ was significantly more negative than $E°(MV^+/MV^0)$ = -0.880 V. Because ε_{MV+} is so large (13,700 $M^{-1}cm^{-1}$) we conservatively estimated the upper limit of $[MV^+]$ throughout the pD 12.8 titration to be 1% of the total added MV^{2+}. Using eqs 1 and 2 and $(MV^0/MV^+ \approx 99/1)$ we calculated the upper limit of $E(TiO_2^{Ox/R})$ to be <-1.0 V at pD 12.8. Thus, the colloids under basic conditions are much more reducing than the acidic TiO_2^R colloids.

To further evaluate $E(TiO_2^{Ox/R})$ over a wide range of pH, *c*-TiO_2^R colloids were titrated with cobaltocenium-1,1'-dicarboxylate ($[Co^{III}(Cp\text{-}COO^-)_2]^-$, abbreviated Co^{III}), and Eu^{III}DTPA (DTPA = diethylenetriamine pentaacetate), in addition to MV^{2+}. The results are summarized in Table 1; the details and data analysis are given in SI-Section 4. Each oxidant was used for multiple experiments over its appropriate range of pH values, depending on its reduction potential and oxidant pH stability (Table S7).

Very similar results were obtained for both MV^{2+} and Co^{III} near pH 5 where both reagents could be used. This is an important confirmation of the robustness of the analysis and the results. In addition, the thermochemistry of *c*-TiO_2^R oxidation is unaffected between a pure-ET oxidant (MV^{2+}) while Co^{III} in this pH range is a PCET oxidant. The Eu(III)DTPA titration suffered from stability concerns, so its uncertainty is larger (Figure 4, green point). The full details of each titration reaction are provided in SI Section 4.

Titrations of *uncapped* TiO_2^R with MV^{2+} at pH ~2 and ~12 gave qualitatively similar results to the citrate capped colloids (Table 1, SI Section 4.1). Under basic conditions, full conversion of MV^{2+} to MV^0 was observed upon reaction with pH 11.7 *uc*-TiO_2^R. At low pH values (2.25 and 2.75), *uc*-TiO_2^R titrated MV^{2+} were only partially reduced to MV^+. At pH ~2.8, the $E(TiO_2^{Ox/R})$ resulting from *c*-TiO_2^R and *uc*-TiO_2^R equilibrations with MV^{2+} differ by only ~60 mV (Table 1). The similarity of the pH ~2.8 reduction potentials for *c*-TiO_2^R and *uc*-TiO_2^R is noteworthy, giv-

en the very different ζ potentials of these colloids, ~0 vs. +40 mV (**Figure 1**).

The data in Table 1 are plotted in **Figure 4**. A linear fit of the *c*-TiO_2 results from MV^{2+} (blue datapoints) and Co^{III} (yellow data) gives a line with a slope of -60 ± 5 mV per pH unit. The two points at high pH were excluded from the fit due to the stability complications mentioned in the previous paragraph, but they are not far from the extrapolated line. The pH 0 intercept gives $E_{pH0}(TiO_2^{Ox/R})$ = –161 ± 31 mV vs NHE.

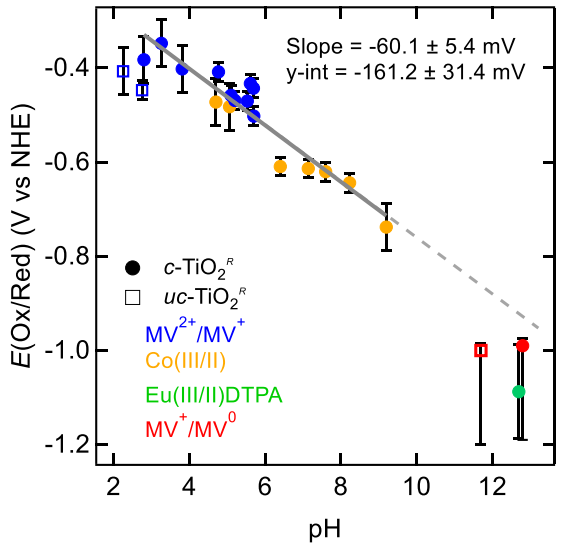

Figure 4. Plot of $E(TiO_2^{Ox/R})$ = *E*(Ox/Red) for the molecular reagent vs. pH. The values are from Table 1: titrations of *c*-TiO_2^R with MV^{2+} (blue and red circles), $[Co^{III}(Cp\text{-}COO^-)_2]^-$ (yellow circles) and Eu^{III}DTPA (green circle), and titrations of *uc*-TiO_2^R with MV^{2+} (blue and red open squares). The points above pH 12 were excluded from the linear fit because of complications in those titrations. [NP] = 20–30 μM, [citric acid] = 4–20 mM, and [e^-] = 0.5–2.0 mM; specific details for each titration are in Table S6.

Table 1. Equilibrations to determine $E(TiO_2^{Ox/R})$.

Ox/Red	pH [a]	[e^-] [b]	[citric acid] [c]	$E(TiO_2^{Ox/R})$ [d]
***c*-TiO_2**				
MV^{2+}/MV^{+} [e]	2.8	1.00	5.7	-0.382
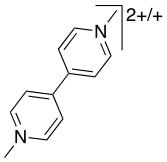	3.3*	0.99	17.0	-0.348
	3.8	1.65	18.5	-0.402
	4.8*	1.00	17.9	-0.408
	5.1	1.00	5.7	-0.458
	5.2	1.00	5.7	-0.469
	5.5	1.00	5.9	-0.470
	5.6	0.34	5.4	-0.433
	5.7	0.50	9.4	-0.502
	5.7	0.42	5.8	-0.443
$Cp'_2Co^{III/II}H_x$ [f]	4.7	1.5	5.65	-0.472
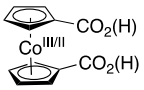	5.06	1.3	5.7	-0.482
	6.4	1.8	5.7	-0.609
	7.14	1.3	5.7	-0.614
	7.6	1.4	5.5	-0.620
	8.23	1.3	5.7	-0.644
	9.2	1.34	5.5	-0.738
$Eu^{III/II}$(DTPA) [g]	12.7	0.7	3.9	-1.09 [h]
MV^+/MV^0 [e]	12.8*	0.9	14.4	<-1.00 [h]
***uc*-TiO_2**				
MV^{2+}/MV^{+} [e]	2.25	0.9		-.407
	2.75	0.9		-.447
MV^+/MV^0 [e]	11.7	0.7		<-1.00 [h]

[a] pH was measured on the bench top after the fully titrated sample was exposed to air. * The measurement is a pD value. See SI-Section 1.7 for details on pD vs. pH. [b] [e^-] in mM. [c] [citric acid] is the pre-photolysis concentration in mM. [d] $E(TiO_2^{Ox/R})$ at different pHs from eqs 1-3. [e] MV^n = methylviologen$^{2+/+/0}$. [f] $Cp'_2Co^{III/II}H_x$ =cobaltocene-1, 1′-dicarboxylic acid, Co^{III} or Co^{II}, with x = 0 (carboxylates) at pH > 5.8 varying protonation states at pH < 5.8 (*E*(Co) varies with pH). [g] Eu^{III}DTPA = Europium(III) diethylenetriamine pentaacetate (SI-Section 4). [h] These values have greater uncertainties (see text).

IV. $E(TiO_2^{Ox/R})$ as a Function of e^-/NP

The equilibrium experiments above focused on the concentrations of the molecular oxidant in its oxidized and reduced forms. In this section, we probe whether the full equilibrium expression for these reactions should also include both the oxidized and reduced populations of TiO_2 (TiO_2^{Ox}, TiO_2^R) (eq 4). In this section, we assume molecule-like behavior equilibrium behavior for the reducing equivalents in TiO_2, equivalent to assuming a Langmuir isotherm. This section also presents experiments at only one pH; a more complete discussion is given below and experiments under other conditions are described in SI Section 4. With molecular behavior of the nano particles, the equilibrium expression for reaction 4 is as shown in eq 5 (ignoring any H^+ dependence, which varies with the oxidant). Eq 5 implies that the measured potential for TiO_2 reduction, $E(TiO_2^{Ox/R})$, should depend on the $[TiO_2^R]/[TiO_2^{Ox}]$ ratio via a version of the Nernst equation (eq 6). Thus, the $[TiO_2^R]/[TiO_2^{Ox}]$ ratio should influence the Ox/Red observed in the equilibration experiments. This effect was not included in the analysis above (eqs 1 and 2) because that involved the non-standard $E(TiO_2^{Ox/R})$ (in common with previous reports of similar experiments[15,35]).

$$TiO_2^R + Ox \rightleftharpoons TiO_2^{Ox} + Red \quad (4)$$

$$K_{eq} = \frac{[TiO_2^{Ox}][Red]}{[TiO_2^R][Ox]} \quad (5)$$

$$E(TiO_2^{Ox/R}) = E^{o\prime}(TiO_2^{Ox/R}) - 59\ mV\ \log\frac{[TiO_2^R]}{[TiO_2^{Ox}]} \quad (6)$$

In order to experimentally probe how the $[TiO_2^{Ox}]/[TiO_2^{R}]$ ratio influences the observed $E(TiO_2^{Ox/R})$, a batch of *c*-TiO_2^{R} was prepared and equilibrated (pH 5.6, 0.44 mM e^-, 9.2 mM citric acid, 26 µM NPs). The batch of *c*-TiO_2^{R} was separated into three different aliquots: (A) unchanged, (B) diluted 10-fold with uncharged *c*-TiO_2 colloid at the same pH, or (C) diluted 10-fold with pH matched H_2O/HCl. All three equilibrated colloids, A–C, were then titrated with methyl viologen (MV^{2+}) to determine the redox potential of each solution (Scheme 2). The measured $E(TiO_2^{Ox}/TiO_2^{R})$ of the stock (A) and the diluted (C) colloids were very similar, -430 and -420 mV respectively, so dilution has little effect. In contrast, the $E(TiO_2^{Ox}/TiO_2^{R})$ of the NP diluted colloid (B) was ~60 mV more positive, -360 mV (Scheme 2).

The similar $E(TiO_2^{Ox}/TiO_2^{R})$ of colloid **A** and the ten-fold diluted **C**, ΔE = 10 mV, is consistent with eq 6. While the absolute concentrations of TiO_2 and e^- differ by 1 order of magnitude between A and C, the ratio $[TiO_2^{Ox}]/[TiO_2^{R}]$ is the same in the two samples. The small 10 mV shift could be due to the dilution of the citrate buffer causing a small change in the surface ligation.

Colloids **B** and **C** contained roughly the same number of additional electrons, $[TiO_2^{R}]$; however, the relative $[TiO_2^{Ox}]$ and average e^-/NP differed by approximately 1 order of magnitude between the two samples. This is due to the addition of uncharged *c*-TiO_2. When probed in the same way with MV^{2+}, the **B** sample was less reducing than **C** by $\Delta E(TiO_2^{Ox}/TiO_2^{R})$ = ~60 mV. This is in excellent agreement with the prediction of the Nernst-type equation 6. This supports the first-order treatment of these TiO_2 NPs by the same thermochemical formalism as for molecules. Some of the complexity glossed over in this section is revisited in Section V of the discussion.

Scheme 2. A *c*-TiO_2^{R} colloid (**A**, pH 5.6, 0.44 mM e^-, 9.2 mM citric acid) was split into 3 batches: (**A**) unchanged (**B**) diluted 10-fold with uncharged, pH-matched TiO_2 colloid, and (**C**) diluted 10-fold with pH-matched H_2O/HCl. $E(TiO_2^{Ox/R})$ calculated after the addition of ([a]) 0.7 µmol MV^{2+} and ([b]) 0.2 µmol MV^{2+}.

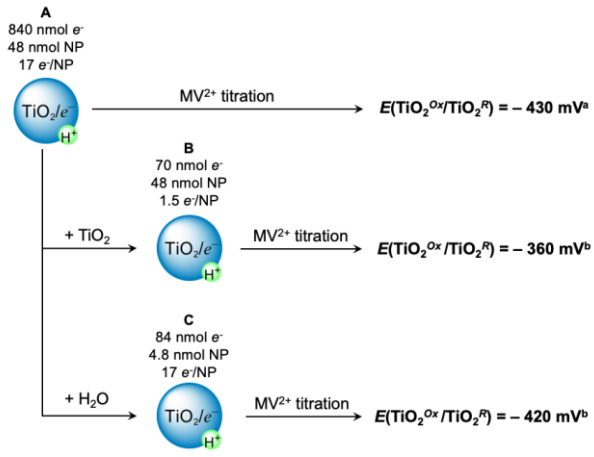

Discussion

I. The preferred reactivity of aqueous TiO_2 is PCET.

Interfacial redox reactions of TiO_2 have been extensively studied for decades, and they are usually described as electron transfer processes. The reaction of TiO_2^{R} with KI_3 in particular has been examined in the context of dye-sensitized solar cells. Yet to our knowledge this is the first demonstration that aqueous TiO_2^{R} colloids *release protons into the solution* when oxidized by an ET oxidant such as KI_3. Analysis of the solvent and pH showed the reaction of TiO_2^{R} with KI_3 released roughly one proton per electron *more* into the solution than the oxidations by PCET oxidants like O_2 and 4-MeO-TEMPO, which accept one proton and one electron. Overall, this analysis shows that an average of slightly more than $1H^+$ per e^- is released in the I_3^- reactions, because even the O_2 and 4-MeO-TEMPO reactions cause some drop in the pH.

This result is important because it shows that $E(TiO_2^{Ox/R})$ and $\Delta G°$ for triiodide oxidation do not simply reflect the energy of an electron in the material. The measured potentials do *not* correspond with electronic energies such as a Fermi energy (E_F), a conduction band edge energy (E_{CB}) or the energetic position of trap state(s) within the band gap. $E(TiO_2^{Ox/R})$ *includes the energy of the proton transfer component*, not just the energetics of the electrons in the material. To use a molecular analogy: the potential for aqueous phenol oxidation to $PhO^{\bullet} + e^- + H^+$ is distinct from the potential for phenoxide (PhO^-) oxidation, the energy of the phenol HOMO orbital, or the phenol ionization energy.

The evidence from this work and prior studies is that proton-coupling of electron transfers is the rule and not the exception for TiO_2. The data show more than the *ability* of TiO_2 to react by PCET, they show that *PCET is the thermodynamically preferred reactivity* of this material, at least over the pH 2-13 range studied. This was the conclusion of Lyon and Hupp twenty years ago for TiO_2 thin films over the normal pH range (though they reported proton-independent behavior at very high and very low proton activities).[16] PCET was also the conclusion by Murray *et al.* for IrO_2 based on the electrochemistry of colloids and films,[52] it is the consensus view of p-type nickel oxide electrodes[55,56] and ruthenium dioxide pseudocapacitors,[29] and it is how we have recently described the reactivity of colloidal ceria NPs.[57] We believe that most redox reactions at the interface of a metal oxide and a protic solution are PCET reactions, despite being typically described by a "pure ET" model.

II. TiO_2^{R} is $TiO_2{\bullet}e^-,H^+$.

The potential (E) for a *molecular* X/XH proton-coupled electron transfer half-reaction shifts by -59 mV per unit pH according to the Nernst equation (eq 7; referenced to NHE, [1M H^+]).[31] The data in Figure 4 show that the 4 ± 1 nm colloidal TiO_2 NPs behave similarly. The -60 ± 5 mV/pH slope of the data shows that the TiO_2 redox couple has equal numbers of electrons and protons. The additional electrons in TiO_2^{R} are coupled to protons in a near 1:1 ratio and the stoichiometry of TiO_2^{R} is roughly $TiO_2{\bullet}e^-,H^+$. The redox process being measured in these equilibrations is shown in eq 8. Combining the $[TiO_2^{R}]/[TiO_2^{Ox}]$ and pH dependences gives the corresponding Nernst equation (eq 9).

$$E(X + e^- + H^+/XH) = E° - 59\ mV\ \log\frac{[XH]}{[X]} - 0.059V \times pH \qquad (7)$$

$$TiO_2 + e^- + H^+ \rightleftharpoons TiO_2{\bullet}e^-,H^+ \qquad (8)$$

$$E(TiO_2^{Ox/R}) \cong E° - 59\ mV\ \log\frac{[TiO_2^{R}]}{[TiO_2^{Ox}]} - 59\ mV \times pH \qquad (9)$$

Many previous studies of TiO_2 thin films have reported that the reduction potential has a slope of a roughly -60 mV/pH.[2,16] Almost 40 years ago, Grätzel, *et al.* reported this slope for colloidal

TiO_2 over a narrow range of pH.[35] The observation here of a -60 mV/pH slope (Figure 4) is not new or surprising, though the range of pH studied is unusually large for colloidal materials. The combination of these data with the stoichiometry of the KI_3 and O_2 reactions (Scheme 1, Figure 2) provides strong evidence that the reactions are PCET. The observation that the KI_3 reaction releases slightly more than one proton per electron is surprising given the -60 mV/pH slope.

III. PCET vs. surface charging: E(TiO_2) and ζ potential.

The traditional explanation of the -60 mV/pH shift of bulk oxide semiconductor potentials is electrostatic charging of the surface. In this explanation, at higher pH, for instance, the oxide surface water and hydroxide groups are deprotonated and therefore the surface is more negatively charged. This electrostatic effect makes it harder to add electrons and the potential becomes more negative. The surface charge is set by the material and the pH, and any number of electrons can be passed through that static interface. The protons and electrons are not stoichiometrically coupled.

This surface-charging model however is not consistent with the observation here that the solution pH drops upon oxidation of a reduced TiO_2 colloid. The release of protons to solution upon oxidation of the NPs requires coupling of the surface protonation to the number of electrons in the material. Lyon and Hupp similarly argued that surface charging could not be the explanation of the -64 mV/pH variation for their TiO_2 thin film, though for a different reason. They observed this linear potential shift over a range of 10^{25} in proton activity, which could not be due to protonation/deprotonation due to the limited number of surface sites.[16]

The ζ potential measurements in the current study (Figure 1) provide independent insights into the NP surface charges. The ζ potential provides the potential at the hydrodynamic slipping plane not the surface charge, but the two are related, typically in a linear relationship.[2,36] In the current study, the ζ potentials for the fully oxidized TiO_2 NPs do not correlate at all with the reduction potential. This is clearly shown by plotting the data in Figure 1 and Figure 4 together vs. the same pH scale (Figure 5) While the reduction potential drops linearly over the whole pH range, the ζ potentials for *c*-TiO_2 drop rapidly from pH 2 to 4, is then fairly constant from ~ pH 5 to 12, and then rise from pH 12 to 14. At high pH when the ζ potential is rising, the TiO_2^R reduction potential keeps dropping and becomes so negative that TiO_2^R fully converts $MV^{\bullet+}$ to MV^0. The absence of a trend between these components is a clear demonstration the reduction potential for *c*-TiO_2 is not moving in response to its ζ potential or surface charge.

Another striking feature of Figure 5 is the comparison of *c*-TiO_2 vs. *uc*-TiO_2 NPs. At pH 2, the ζ potentials are quite different: ~0 mV for the citrate-capped and ca. +40 mV for the uncapped. Yet the *uc*- and *c*-TiO_2 reduction potentials are very similar at low pH. At high pH ~12, the ζ potentials are similar at ca. –50 mV, and the reduction potentials are similar. As in the prior paragraph, there is no correspondence between the ζ potentials and the reduction potentials.

These data support the conclusion that redox reactions involve the transfer of $1e^-$ and $1H^+$, eq 8. Because there is no net charge being transferred, there is no significant electrostatic effect on the reduction potential. The lack of correlation between $E(\zeta)$ and $E(TiO_2/TiO_2{\bullet}e^-,H^+)$ is contrary to the predictions of the surface charging model for the shift in reduction potentials, but consistent with the PCET conclusion.

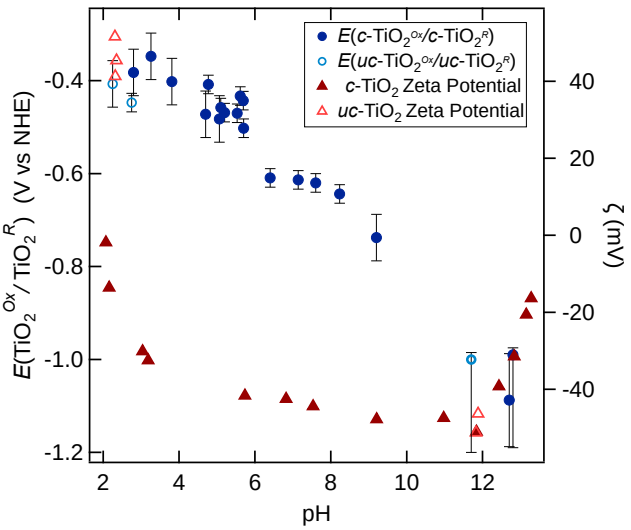

Figure 5. Plot of $E(TiO_2^{Ox/R})$ (left axis, circles) and ζ potential (right axis, triangles) vs pH, an overlay of data from Figure 1 and Figure 4. ζ Potentials are mostly for *c*-TiO_2 (filled triangles) with a few values for *uc*-TiO_2 (unfilled triangles) at low and high pH. $E(TiO_2^{Ox/R})$ values (Table 1) are mostly for *c*-TiO_2 (filled circles) with a few values for *uc*-TiO_2 (unfilled circles) at low and high pH.

IV. The TiO_2^R–H Bond Dissociation Free Energy (BDFE).

For a molecular compound, the $1e^-/1H^+$ X/XH standard reduction potential is equivalent to the X–H Bond Dissociation Free Energy (BDFE), following Scheme 3 and eq 10.[31,32] This is because a proton plus an electron is thermodynamically equivalent to a hydrogen atom via the constant C_G. Our lab has recently shown that the same cycle applies to nickel oxide electrodes,[56] and Jackson, Pegis and Surendranath have shown that a version of it can be applied to functionalized carbon electrodes.[58]

Scheme 3. Relationship between $E°$(X/XH) and BDFE(XH).[31,32]

$$X + H^+ + e^- \xrightarrow{E°(X/XH)} XH$$
$$H^\bullet \xrightarrow{C_G} H^+ + e^-$$
$$X + H^\bullet \xrightarrow{BDFE(XH)} XH$$

$$BDFE(X–H) = 23.06E°(X/XH) + C_G \quad (10)$$

$$BDFE(TiO_2^R–H) = 23.06E°(TiO_2/TiO_2{\bullet}e^-,H^+) + C_G \quad (11)$$

Applying Scheme 3 to colloidal TiO_2 gives eq 11, which requires C_G (52.8 kcal mol^{-1})[32,59] and the pH 0 intercept of the $E(TiO_2^{Ox/R})$ line in Figure 4: –161 ± 31 mV vs NHE. These values yield a BDFE for TiO_2^R–H of 49 ± 2 kcal mol^{-1} (the uncertainty deriving both from the measurements and from the value of C_G).

The TiO_2^R–H BDFE of 49 ± 2 kcal mol^{-1} is quite low. It indicates that TiO_2^R–H should thermodynamically be able to liberate H_2, as the BDFE is less than C_G. As confirmation of this, placing a piece of platinum metal in a solution of $TiO_2{\bullet}e^-,H^+$ causes decoloration of the blue colloid and the appearance of bubbles—presumably H_2—on the electrode. This result was expected also

because $E(TiO_2^{Ox/R})$ is below the reversible hydrogen electrode (RHE) ($E_{pH0}(TiO_2^{Ox/R})$ = –161 ± 31 mV vs NHE; Figure 4).

The BDFE(TiO_2^R–H) of 49 ± 2 kcal mol^{-1} is less than half the BDFE(HO–H) of water in water, 115.8 kcal mol^{-1}.[32] The 49 ± 2 kcal mol^{-1} BDFE is, however, close to the computed bond enthalpy for water bound to a molecular Ti^{3+} center, Cp_2ClTi(HO–H), 49.4 kcal mol^{-1} [60] (the BDFE in the gas phase is typically ~8 kcal mol^{-1} smaller than the BDE[32]). Such 'coordination-induced bond weakening' has become common in molecular coordination chemistry but to our knowledge this weak (TiO_2^R–H) bond is the first time this concept has been connected to a materials interface. [61] It should be a common effect for surfaces that have surface H and can easily be oxidized.

A recent theoretical study provided a more atomistic view of this BDFE, considering two different types of surface e^-/H^+ polaron trap states in a periodic anatase TiO_2 slab.[61] The computations also find a very weak O–H bond, 39 kcal mol^{-1}, associated with in $Ti^{3+}OH^-$ polaron defects. This study is consistent with the view that these BDFEs can be simply viewed as the removal of a proton from a surface hydroxide and an electron from a Ti^{3+} ion,[31,32,61] as illustrated in Scheme 4.

Scheme 4. Simplified schematic of the TiO_2–H

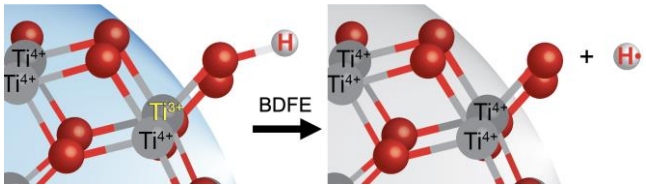

V. Multiple redox equivalents in TiO_2 nanoparticles.

The Discussion so far has assumed that all of the electrons (H-atoms) in reduced TiO_2 NPs are equivalent, that there is a single value of $E(TiO_2/TiO_2{\bullet}e^-,H^+)$ at a given pH and a single TiO_2–H BDFE. However, TiO_2 has multiple types of trap states and possible protonation sites BDFE. sites (bridging terminal, lattice oxides/hydroxides), and the colloids studied here have on average 10-60 electrons (H$^\bullet$) per NP. It is not required that the first reducing equivalent has the same properties as the last, and it is likely the NPs studied here contain a distribution of sites. As Grätzel described in a review 35 years ago (using the electron-only model for reduction):[35,62]

> "It might be expected that the storage of 300 electrons in a 50 Å-sized particle would produce a large negative shift in its potential with respect to the surrounding aqueous solution. However, the TiO_2/water interface is distinguished by a large double layer capacity, which is 85 μF cm^{-2} at the point of zero charge and increases to 200-300 μF cm^{-2} in alkaline solution.[63] The negative shift in the potential of the particle during accumulation of 300 electrons is therefore only 25 to 90 mV."

The data reported here similarly show that there are only small differences in the thermochemistry of the many trapped electrons. The ~60 mV shift upon 10-fold dilution of the TiO_2^R with TiO_2 (Results Section IV) is what would be expected simply as a results of mass action. This is the same as diluting a solution of a molecular reductant—where all the molecules are identical—with its oxidized form. The small shift of the reduction potentials with the amount of charging is also evident in the close potentials measured by titrations with MV^{2+} or Co^{III} at pH ~5. The MV^{2+} reactions only removed a few percent of the reducing equivalents in the NPs while the Co^{III} titrations proceeded essentially to completion, removing all ~50 electrons. Yet the potential measured with Co^{III} at pH 5.06 is only 24 mV more negative than that measured with MV^{2+} at pH 5.1.

While our experimental data and those of Grätzel agree quite well, our interpretation is different. Capacitance would not seem to be the correct model because there is little charge accumulation on the NPs. The addition and removal of electrons are charge-compensated by proton transfers. The chemistry occurring is best described as the net addition or removal of neutral hydrogen atoms. This is consistent with the potential and BDFE(TiO_2–H) being very similar for *c*-TiO_2 and *uc*-TiO_2 despite their sizable difference in ζ potential (Figure 5). This charge balancing likely contributes to the stability of highly reduced 'charged' NPs.

The *uc*-TiO_2^R NPs used here have two distinct classes of trap states that are in equilibrium, which have different optical and EPR spectra, and different kinetic reactivities.[13,14] The citrate-capped *c*-TiO_2^R have a spectroscopically different pattern of occupied trap states.[13] More generally, different types of reduced TiO_2 have various ill-defined trap states, often involving the electron on a small clusters of Ti ions.[7,13,14,60,64-69] Still, this heterogeneity does not lead to substantial diversity of potentials or BDFEs. For instance, the potentials and BDFEs for the capped and uncapped TiO_2 NPs are quite similar, even though the trap states and ζ potentials are different.

A similar conclusion of a narrow distribution of trap state energies—BDFEs—was recently reported for different reduced TiO_2 NPs. This study used oleate-ligated NPs in toluene, and it probed a more subtle energy scale.[70] This narrow distribution of BDFEs is not a general result for oxide NPs, however. For oleate-capped ceria NPs, $CeO_{2-x}H_y$, the surface O–H BDFEs vary by 13 kcal mol^{-1} (0.56 eV) as a function of the % reduction of those nanocrystals.[57]

The similar properties of the multiple electrons in the reduced TiO_2 NPs is what allows the use of a molecular treatment, such as the Nernst-type eq 9. If there were attractive or repulsive interactions between the H's on the NP, or a thermochemically diverse set of sites, this treatment would not hold. In the language of surface science, the isotherm for H binding is close to the Langmuir isotherm. Perhaps one reason why the properties of the different trap states are similar is that the NPs are charged to only between 0.01 and 0.06 e^-/Ti atom, or 1e^- per 13-100 Ti atoms, and are thus likely somewhat separated. Still, the density of added electrons is quite high in these NPs, ca. 10^{21} cm^{-3}.

While the description of these reduced TiO_2 NPs as similar to molecules is powerful, the analogy is not perfect. We close this section by highlighting one particular complexity. The Nernst equation and Langmuir isotherm analyses require the concentration of unfilled (empty) states, [TiO_2^{Ox}], not only the concentration of filled states ([TiO_2^R]). Unfortunately, the number of possible empty trap or conduction band states per NP is not known, as [TiO_2^{ox}] is not the same as [TiO_2^R]–[Ti]$_{total}$. The concentration of unfilled sites could vary with the potential of the reductant or energy scale being probed. The uncertainty in the [TiO_2^{Ox}] means that the standard potential $E°(TiO_2^{Ox/R})$ in eqs 6 and 9 is not well defined. In a normal Nernst treatment, the standard state would be defined as equal concentrations of filled and unfilled states. For a Langmuir isotherm, the standard state is similarly a surface coverage of 0.5 (equal number of filled and unfilled sites). For the NPs used here, the experimentally attainable charging limit is ca. one H-atom per 30 Ti atoms, and the *E*"°" in this report uses a quasi-reference state that is roughly half of that.

Conclusions and Implications

The experiments in this report show that equilibrated redox reactions at aqueous, colloidal TiO_2 occur by proton-coupled electron transfer (PCET) over the pH range 2-13. This conclusion goes beyond the statement that TiO_2 *can* undergo PCET to state that PCET is the thermodynamically preferred mode of reactivity.

This conclusion is indicated by the release of protons from reduced NPs upon their oxidation with the electron-only oxidant KI_3. The approximately 1:1 coupling of electrons and protons in reduced TiO_2 is also indicated by the shift in the reduction potential of –60 ± 5 mV per unit change in pH, between pH 2 and >9. Thus, the reduction potential should be described as $E(TiO_2/TiO_2{\bullet}e^-,H^+)$.

The roughly $1e^-$:$1H^+$ stoichiometry means that little net charge is added or removed from the TiO_2 in these redox reactions, and that the net chemistry can alternatively be described as hydrogen atom transfer (HAT): $TiO_2 + H^\bullet \rightarrow TiO_2–H$. This perspective explains the insensitivity of the reduction potentials to the measured ζ potentials of the colloid, and to the presence or absence of citrate capping ligands. The standard $1e^-$:$1H^+$ reduction potential of –161 ± 31 mV vs NHE implies a $TiO_2–H$ bond dissociation free energy (BDFE) of 49 ± 2 kcal mol^{-1}. This can be identified as an example of the molecular effect of 'coordination induced bond weakening'[32,59] at a material interface.

We believe the conclusion of preferred PCET reactivity is general for aqueous TiO_2 interfaces. In fact, we know of no equilibrated potential measurement for a TiO_2|aqueous interface that has been shown *not* to be proton-coupled. Taking these results together with related studies of nickel oxide and ceria,[56,57] we suggest that the conclusions of preferred redox reactivity by PCET will prove to be quite general for interfaces between oxide materials and protic solutions. Future studies will examine the kinetics and mechanistic distinctions of the PCET reactivity, concerted e^-/H^+ transfer vs. stepwise ET then PT or PT then ET.

Finally, we emphasize that the measured PCET energies do *not* correspond to "electronic energies" of the TiO_2.[61,71] It is very common in the literature to equate a reduction potential such as $E_{pH0}(TiO_2^{Ox/R})$ to the semiconductor Fermi energy, flat-band potential, conduction band edge energy, or trap state energy. However, *that correspondence is not appropriate if the E refers to a PCET process*.[71] PCET processes include contributions from both the transfer of the electron and the transfer of the proton.[32] To make a molecular analogy, the potential for $H^+ + e^- = ½H_2$ does not correspond to any "electronic energy" in H_2 (g) or aqueous H^+ (or H_3O^+). In this sense, colloidal TiO_2 behaves like a dissolved molecular PCET reagent.

ASSOCIATED CONTENT

Supporting Information

Experimental details including synthesis and characterization of TiO_2 nanoparticles, both uncapped and citrate-capped and both as-prepared and reduced, and equilibrations with various oxidants. This material is available free of charge via the Internet at http://pubs.acs.org.

AUTHOR INFORMATION

Corresponding Author

*E-mail: james.mayer@yale.edu

Notes

The authors declare no competing financial interest.

Funding Sources

This work was funded by the U.S. Department of Energy, Office of Science, Basic Energy Sciences and the US-Israel Binational Science Foundation Grant as described in the Acknowledgement. B.B. was supported by the Frontiers in Chemistry Masters Program at the University of Paris.

ACKNOWLEDGMENT

We acknowledge primary support first from the Center for Light Energy Activated Redox Processes (LEAP), an Energy Frontier Research Center funded by the U.S. Department of Energy, Office of Science, Basic Energy Sciences, under Award No. DESC0001059, and subsequently from the U.S. Department of Energy, Office of Science, Basic Energy Sciences, under Award No. DESC0021298. Funding for this project was also provided by the US-Israel Binational Science Foundation Grant BSF No. 2016123. We are grateful to the Frontiers in Chemistry Masters Program at the University of Paris for supporting B.B.'s extended visit to Yale. Zeta potential measurements were performed in the Facility for Light Scattering at Yale University, and we thank Dr. Sara Hashmi for her assistance with these measurements. We also acknowledge helpful conversations with Prof. Ira Weinstock, Sapir Dabush-Avnaim, and Dr. Rishi Agarwal.

References and Endnotes

1. Fierro, J. L. G., *Metal oxides : chemistry and applications*. CRC Taylor & Francis: Boca Raton, FL, 2006.
2. Finklea, H. O., Titanium Dioxide (TiO_2) and Strontium Titanate ($SrTiO_3$). In *Semiconductor Electrodes*, Finklea, H. O., Ed. Elsevier: Amsterdam, 1988; pp 42–154.
3. Hoffmann, M. R.; Martin, S. T.; Choi, W.; Bahnemann, D. W., Environmental Applications of Semiconductor Photocatalysis. *Chem. Rev.* **1995,** *95*, 69-96.
4. Kalyanasundaram, K.; Grätzel, M.; Pelizzetti, E., Interfacial electron transfer in colloidal metal and semiconductor dispersions and photodecomposition of water. *Coord. Chem. Rev.* **1986,** *69*, 57-125.
5. Ma, Y.; Wang, X.; Jia, Y.; Chen, X.; Han, H.; Li, C., Titanium Dioxide-Based Nanomaterials for Photocatalytic Fuel Generations. *Chem. Rev.* **2014,** *114*, 9987-10043.
6. Bourikas, K.; Kordulis, C.; Lycourghiotis, A., Titanium Dioxide (Anatase and Rutile): Surface Chemistry, Liquid–Solid Interface Chemistry, and Scientific Synthesis of Supported Catalysts. *Chem. Rev.* **2014,** *114*, 9754-9823.
7. Schneider, J.; Matsuoka, M.; Takeuchi, M.; Zhang, J.; Horiuchi, Y.; Anpo, M.; Bahnemann, D. W., Understanding TiO_2 Photocatalysis: Mechanisms and Materials. *Chem. Rev.* **2014,** *114*, 9919-9986.
8. Habisreutinger, S. N.; Schmidt-Mende, L.; Stolarczyk, J. K., Photocatalytic Reduction of CO_2 on TiO_2 and Other Semiconductors. *Angew. Chem. Int. Ed.* **2013,** *52*, 7372-7408.
9. Nowotny, J., *Oxide Semiconductors for Solar Energy Conversion: Titanium Dioxide* CRC Press: New York, 2012.
10. Morrison, S. R., The Solid/Liquid Interface. In *Electrochemistry at Semiconductor and Oxidized Metal Electrodes*, Plenum Press: New York, NY, 1980; pp 49-75.
11. Nozik, A. J., Photoelectrochemistry: Applications to Solar Energy Conversion. *Annu. Rev. Phys. Chem.* **1978,** *29*, 189-222.
12. Mohamed, H. H.; Mendive, C. B.; Dillert, R.; Bahnemann, D. W., Kinetic and Mechanistic Investigations of Multielectron Transfer Reactions Induced by Stored Electrons in TiO_2 Nanoparticles: A Stopped Flow Study. *J. Phys. Chem. A* **2011,** *115*, 2139-2147.
13. Peper, J. L.; Vinyard, D. J.; Brudvig, G. W.; Mayer, J. M., Slow Equilibration between Spectroscopically Distinct Trap States in Reduced TiO_2 Nanoparticles. *J. Am. Chem. Soc.* **2017,** *139*, 2868-2871.
14. Peper, J. L.; Gentry, N. E.; Brezny, A. C.; Field, M. J.; Green, M. T.; Mayer, J. M., Different Kinetic Reactivities of Electrons in Distinct TiO_2 Nanoparticle Trap States. *J. Phys. Chem. C* **2021,** *125*, 680-690.
15. Dimitrijevic, N. M.; Savic, D.; Mićić, O. I.; Nozik, A. J., Interfacial electron-transfer equilibria and flatband potentials of α-Fe_2O_3 and TiO_2 colloids studied by pulse radiolysis. *J. Phys. Chem.* **1984,** *88*, 4278-4283.
16. Lyon, L. A.; Hupp, J. T., Energetics of the Nanocrystalline Titanium Dioxide/Aqueous Solution Interface: Approximate Conduction Band Edge Variations between $H_0 = -10$ and $H_- = +26$. *J. Phys. Chem. B* **1999,** *103*, 4623-4628.

17. Lemon, B. I.; Hupp, J. T., Photochemical Quartz Crystal Microbalance Study of the Nanocrystalline Titanium Dioxide Semiconductor Electrode/Water Interface: Simultaneous Photoaccumulation of Electrons and Protons. *J. Phys. Chem.* **1996,** *100*, 14578-14580.
18. Lemon, B. I.; Hupp, J. T., Electrochemical Quartz Crystal Microbalance Studies of Electron Addition at Nanocrystalline Tin Oxide/Water and Zinc Oxide/Water Interfaces: Evidence for Band-Edge-Determining Proton Uptake. *J. Phys. Chem. B* **1997,** *101*, 2426-2429.
19. Ramamurthy, V.; Schanze, K. S.; Gaal, D. A.; Hupp, J. T., Photo-Induced Electron Transfer Reactivity at Nanoscale Semiconductor- Solution Interfaces: Case Studies with Dye-Sensitized SnO_2-Water Interfaces. In *Semiconductor Photochemistry And Photophysics*, Ramamurthy, V. S., Kirk S., Ed. Marcel Dekker: New York, 2003; Vol. 10.
20. McCool, N. S.; Swierk, J. R.; Nemes, C. T.; Saunders, T. P.; Schmuttenmaer, C. A.; Mallouk, T. E., Proton-Induced Trap States, Injection and Recombination Dynamics in Water-Splitting Dye-Sensitized Photoelectrochemical Cells. *ACS Appl. Mater. Interfaces* **2016,** *8*, 16727-16735.
21. Halverson, A. F.; Zhu, K.; Erslev, P. T.; Kim, J. Y.; Neale, N. R.; Frank, A. J., Perturbation of the Electron Transport Mechanism by Proton Intercalation in Nanoporous TiO_2 Films. *Nano Lett.* **2012,** *12*, 2112-2116.
22. Swierk, J. R.; McCool, N. S.; Saunders, T. P.; Barber, G. D.; Mallouk, T. E., Effects of Electron Trapping and Protonation on the Efficiency of Water-Splitting Dye-Sensitized Solar Cells. *J. Am. Chem. Soc.* **2014,** *136*, 10974-10982.
23. Boschloo, G.; Fitzmaurice, D., Electron Accumulation in Nanostructured TiO_2 (Anatase) Electrodes. *J. Phys. Chem. B* **1999,** *103*, 7860-7868.
24. Koelle, U.; Moser, J.; Graetzel, M., Dynamics of Interfacial Charge-Transfer Reactions in Semiconductor Dispersions. Reduction of Cobaltoceniumdicarboxylate in Colloidal Titania. *Inorg. Chem.* **1985,** *24*, 2253-2258.
25. Ginley, D. S.; Knotek, M. L., Hydrogen in TiO_2 Photoanodes. *J. Electrochem. Soc.* **1979,** *126*, 2163-2166.
26. Brant, A. T.; Yang, S.; Giles, N. C.; Halliburton, L. E., Hydrogen donors and Ti^{3+} ions in reduced TiO_2 crystals. *J. Appl. Phys.* **2011,** *110*, 053714.
27. Kim, Y.-S.; Kriegel, S.; Harris, K. D.; Costentin, C.; Limoges, B.; Balland, V., Evidencing Fast, Massive, and Reversible H^+ Insertion in Nanostructured TiO_2 Electrodes at Neutral pH. Where Do Protons Come From? *J. Phys. Chem. C* **2017,** *121*, 10325-10335.
28. Kim, Y. S.; Balland, V.; Limoges, B.; Costentin, C., Cyclic voltammetry modeling of proton transport effects on redox charge storage in conductive materials: application to a TiO_2 mesoporous film. *Phys. Chem. Chem. Phys.* **2017,** *19*, 17944-17951.
29. Fleischmann, S.; Mitchell, J. B.; Wang, R.; Zhan, C.; Jiang, D.-e.; Presser, V.; Augustyn, V., Pseudocapacitance: From Fundamental Understanding to High Power Energy Storage Materials. *Chem. Rev.* **2020,** *120*, 6738-6782.
30. McCarthy, B. D.; Dempsey, J. L., Decoding Proton-Coupled Electron Transfer with Potential–pK_a Diagrams. *Inorg. Chem.* **2017,** *56*, 1225-1231.
31. Warren, J. J.; Tronic, T. A.; Mayer, J. M., Thermochemistry of Proton-Coupled Electron Transfer Reagents and its Implications. *Chem. Rev.* **2010,** *110*, 6961-7001.
32. Agarwal, R. G.; Coste, S. C.; Groff, B. D.; Heuer, A. M.; Noh, H.; Parada, G. A.; Wise, C. F.; Nichols, E. M.; Warren, J. J.; Mayer, J. M., Free Energies of Proton-Coupled Electron Transfer Reagents and Their Applications. *Chem. Rev.* **2021,** *Accepted*.
33. Pourbaix, M., *Atlas of electrochemical equilibria in aqueous solutions*. National Association of Corrosion Engineers: Houston, Tex., 1974.
34. Pourbaix, M. J. N.; Zoubov, N. d., *Atlas D'equilibres Électrochimiques*. Gauthier-Villars: Paris, 1963.
35. Dung, D.; Ramsden, J.; Grätzel, M., Dynamics of interfacial electron-transfer processes in colloidal semiconductor systems. *J. Am. Chem. Soc.* **1982,** *104*, 2977-2985.
36. Doane, T. L.; Chuang, C.-H.; Hill, R. J.; Burda, C., Nanoparticle ζ -Potentials. *Acc. Chem. Res.* **2012,** *45*, 317-326.
37. Kaszuba, M.; Corbett, J.; Watson, F. M.; Jones, A., High-Concentration Zeta Potential Measurements Using Light-Scattering Techniques. *Philos. Trans. Royal Soc. A* **2010,** *368*, 4439-4451.
38. Covington, A. K.; Paabo, M.; Robinson, R. A.; Bates, R. G., Use of the glass electrode in deuterium oxide and the relation between the standardized pD (paD) scale and the operational pH in heavy water. *Anal. Chem.* **1968,** *40*, 700-706.
39. Glasoe, P. K.; Long, F. A., Use of Glass Electrodes to Measure Acidities in Deuterium Oxide. *J. Phys. Chem.* **1960,** *64*, 188-190.
40. Mikkelsen, K.; Nielsen, S. O., Acidity Measurements with the Glass Electrode in H_2O-D_2O Mixtures. *J. Phys. Chem.* **1960,** *64*, 632-637.
41. Krężel, A.; Bal, W., A formula for correlating pK_a values determined in D_2O and H_2O. *J. Inorg. Biochem.* **2004,** *98*, 161-166.
42. Kormann, C.; Bahnemann, D. W.; Hoffmann, M. R., Preparation and characterization of quantum-size titanium dioxide. *J. Phys. Chem.* **1988,** *92*, 5196-5201.
43. Fernández-Nieves, A.; Nieves, F. J.; Richter, C., Point of zero charge estimation for a TiO_2/water interface. In *Trends in Colloid and Interface Science XII*, Koper, G. J. M.; Bedeaux, D.; Cavaco, C.; Sager, W. F. C., Eds. Steinkopff: Darmstadt, 1998; Vol. 110, pp 21-24.
44. Mudunkotuwa, I. A.; Grassian, V. H., Citric Acid Adsorption on TiO_2 Nanoparticles in Aqueous Suspensions at Acidic and Circumneutral pH: Surface Coverage, Surface Speciation, and Its Impact on Nanoparticle−Nanoparticle Interactions. *J. Am. Chem. Soc.* **2010,** *132*, 14986-14994.
45. Augugliaro, V.; Bellardita, M.; Loddo, V.; Palmisano, G.; Palmisano, L.; Yurdakal, S., Overview on Oxidation Mechanisms of Organic Compounds by TiO_2 in Heterogeneous Photocatalysis. *J. Photochem. Photobiol. C* **2012,** *13*, 224-245.
46. Panayotov, D. A.; Burrows, S. P.; Morris, J. R., Photooxidation Mechanism of Methanol on Rutile TiO_2 Nanoparticles. *J. Phys. Chem. C* **2012,** *116*, 6623-6635.
47. Meichtry, J. M.; Quici, N.; Mailhot, G.; Litter, M. I., Heterogeneous photocatalytic degradation of citric acid over TiO_2: II. Mechanism of citric acid degradation. *Appl. Catal. B* **2011,** *102*, 555-562.
48. Ji, Y.; Wang, B.; Luo, Y., A Comparative Theoretical Study of Proton-Coupled Hole Transfer for H_2O and Small Organic Molecules (CH_3OH, HCOOH, H_2CO) on the Anatase TiO_2(101) Surface. *J. Phys. Chem. C* **2014,** *118*, 21457-21462.
49. Schrauben, J. N.; Hayoun, R.; Valdez, C. N.; Braten, M.; Fridley, L.; Mayer, J. M., Titanium and Zinc Oxide Nanoparticles Are Proton-Coupled Electron Transfer Agents. *Science* **2012,** *336*, 1298-1301.
50. Sheng, H.; Ji, H.; Ma, W.; Chen, C.; Zhao, J., Direct Four-Electron Reduction of O_2 to H_2O on TiO_2 Surfaces by Pendant Proton Relay. *Angew. Chem. Int. Ed.* **2013,** *52*, 9686-9690.
51. Seraghni, N.; Belattar, S.; Mameri, Y.; Debbache, N.; Sehili, T., Fe(III)-Citrate-Complex-Induced Photooxidation of 3-Methylphenol in Aqueous Solution. *Int. J. Photoenergy* **2012,** *2012*, e630425.
52. Gambardella, A. A.; Bjorge, N. S.; Alspaugh, V. K.; Murray, R. W., Voltammetry of Diffusing 2 nm Iridium Oxide Nanoparticles. *J. Phys. Chem. C* **2011,** *115*, 21659-21665.
53. Lyons, M. E. G.; Doyle, R. L.; Godwin, I.; O'Brien, M.; Russell, L., Hydrous Nickel Oxide: Redox Switching and the Oxygen Evolution Reaction in Aqueous Alkaline Solution. *J. Electrochem. Soc.* **2012,** *159*, H932-H944.
54. Stoerzinger, K. A.; Rao, R. R.; Wang, X. R.; Hong, W. T.; Rouleau, C. M.; Shao-Horn, Y., The Role of Ru Redox in pH-Dependent Oxygen Evolution on Rutile Ruthenium Dioxide Surfaces. *Chem* **2017,** *2*, 668-675.
55. Bode, H.; Dehmelt, K.; Witte, J., Zur Kenntnis der Nickelhydroxidelektrode. II. Über die Oxydationsprodukte von Nickel(II)-hydroxiden. *Z. Anorg. Allg. Chem.* **1969,** *366*, 1-21.
56. Wise, C. F.; Mayer, J. M., Electrochemically Determined O–H Bond Dissociation Free Energies of NiO Electrodes Predict Proton-Coupled Electron Transfer Reactivity. *J. Am. Chem. Soc.* **2019,** *141*, 14971-14975.
57. Agarwal, R. G.; Kim, H.-J.; Mayer, J. M., Nanoparticle O–H Bond Dissociation Free Energies from Equilibrium Measurements of Cerium Oxide Colloids. *J. Am. Chem. Soc.* **2021,** *143*, 2896-2907.

58. Jackson, M. N.; Pegis, M. L.; Surendranath, Y., Graphite-Conjugated Acids Reveal a Molecular Framework for Proton-Coupled Electron Transfer at Electrode Surfaces. *ACS Cent. Sci.* **2019,** *5*, 831-841.
59. Connelly, S. J.; Wiedner, E. S.; Appel, A. M., Predicting the reactivity of hydride donors in water: thermodynamic constants for hydrogen. *Dalton Trans.* **2015,** *44*, 5933-5938.
60. Paradas, M.; Campaña, A. G.; Jiménez, T.; Robles, R.; Oltra, J. E.; Buñuel, E.; Justicia, J.; Cárdenas, D. J.; Cuerva, J. M., Understanding the Exceptional Hydrogen-Atom Donor Characteristics of Water in Ti^{III}-Mediated Free-Radical Chemistry. *J. Am. Chem. Soc.* **2010,** *132*, 12748-12756.
61. Warburton, R. E.; Mayer, J. M.; Hammes-Schiffer, S., Proton-Coupled Defects Impact O–H Bond Dissociation Free Energies on Metal Oxide Surfaces. *J. Phys. Chem. Lett.* **2021**, 9761-9767.
62. Grätzel's TiO2 NPs referred to in this quote were slightly larger (5 vs. 4 nm) and had ca. five-fold higher electron density than the materials examined in the current study.
63. Healy, T. W.; White, L. R., Ionizable surface group models of aqueous interfaces. *Adv. Colloid Interface Sci.* **1978,** *9*, 303-345.
64. Rex, R. E.; Knorr, F. J.; McHale, J. L., Surface Traps of TiO_2 Nanosheets and Nanoparticles as Illuminated by Spectroelectrochemical Photoluminescence. *J. Phys. Chem. C* **2014,** *118*, 16831-16841.
65. Berger, T.; Sterrer, M.; Diwald, O.; Knözinger, E.; Panayotov, D.; Thompson, T. L.; Yates, J. T., Light-Induced Charge Separation in Anatase TiO_2 Particles. *J. Phys. Chem. B* **2005,** *109*, 6061-6068.
66. Ghosh, A. K.; Wakim, F. G.; Addiss, R. R., Photoelectronic Processes in Rutile. *Phys. Rev.* **1969,** *184*, 979-988.
67. Howe, R. F.; Grätzel, M., EPR Observation of Trapped Electrons in Colloidal TiO_2. *The Journal of Physical Chemistry* **1985,** *89*, 4495-4499.
68. Rajh, T.; Nedeljkovic, J. M.; Chen, L. X.; Poluektov, O.; Thurnauer, M. C., Improving Optical and Charge Separation Properties of Nanocrystalline TiO_2 by Surface Modification with Vitamin C. *J. Phys. Chem. B* **1999,** *103*, 3515-3519.
69. Kohtani, S.; Kawashima, A.; Miyabe, H., Reactivity of Trapped and Accumulated Electrons in Titanium Dioxide Photocatalysis. *Catalysts* **2017,** *7*, 303.
70. Castillo-Lora, J.; Mitsuhashi, R.; Mayer, J. M., Revealing the Relative Electronic Landscape of Colloidal ZnO and TiO_2 Nanoparticles via Equilibration Studies. *J. Phys. Chem. C* **2019,** *123*, 10262-10271.
71. Peper, J. L.; Mayer, J. M., Manifesto on the Thermochemistry of Nanoscale Redox Reactions for Energy Conversion. *ACS Energy Lett.* **2019**, 866-872.

Table of Contents Graphic:

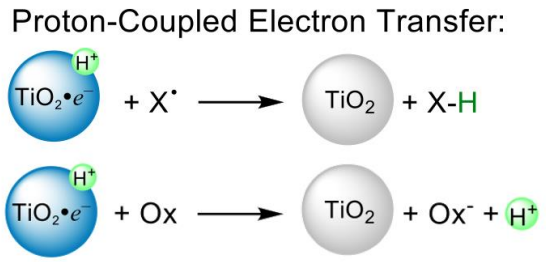

Synopsis text to accompany TOC Graphic:

Aqueous colloidal TiO_2 nanoparticles have a thermodynamic preference to react by proton-coupled electron transfer (PCET), and they behave like molecular $1e^-/1H^+$ redox couples. This means that the measured $E(TiO_2/TiO_2{\bullet}e^-,H^+)$ is not a semiconductor electronic energy but rather corresponds to a TiO_2–H bond dissociation free energy (BDFE = 49 ± 2 kcal mol^{-1}).